Phosphorescent Cationic Iridium(III) Complexes Bearing a Nonconjugated Six-Membered Chelating Ancillary Ligand: A Strategy for Tuning the Emission Towards the Blue

Supporting Information

Claus Hierlinger,[a,b] David B. Cordes,[b] Alexandra M. Z. Slawin,[b] Denis Jacquemin*,[c] Véronique Guerchais*,[a] Eli Zysman-Colman*[b]

[a] Univ Rennes, CNRS, ISCR (Institut des Sciences Chimiques de Rennes) – UMR 6226, F-35000 Rennes, France. *E-mail: veronique.guerchais@univ-rennes1.fr; Tel: + 33 (0)2 23 23 67 29; Fax : + 33(0) 23 23 69 39*

[b] *Organic Semiconductor Centre, EaStCHEM School of Chemistry, University of St Andrews, St Andrews, Fife, KY16 9ST, UK. E-mail: eli.zysman-colman@st-andrews.ac.uk; Web: http://www.zysman-colman.com; Tel: +44 (0)1334 463826; Fax: +44 (0)1334 463808.*

[c] *UMR CNRS 6230, Université de Nantes, CEISAM, 2 rue de la Houssinière, 44322 Nantes Cedex 3, France*

Table of Contents

Experimental Section

General Synthetic Procedures

Commercial chemicals were used as supplied. All reactions were performed using standard Schlenk techniques under inert (N_2) atmosphere with reagent-grade solvents. Flash column chromatography was performed using silica gel (Silia-P from Silicycle, 60 Å, 40-63 μm). Analytical thin layer chromatography (TLC) was performed with silica plates with aluminum backings (250 μm with indicator F-254). Compounds were visualized under UV light. ^{1}H, ^{13}C, ^{19}F and ^{31}P solution-phase NMR spectra were recorded on a Bruker Avance 400 and 500 Mhz spectrometers. The following abbreviations have been used for multiplicity assignments: "s" for singlet, "d" for doublet, "t" for triplet, "m" for multiplet and "br" for broad. ^{1}H and ^{13}C NMR spectra were referenced to the solvent peak. Melting points (Mps) were recorded using open-ended capillaries on an electrothermal melting point apparatus and are uncorrected. High-resolution mass spectra were recorded at the EPSRC UK National Mass Spectrometry Facility at Swansea University on a quadrupole time-of-flight (ESI-Q-TOF), model ABSciex 5600 Triple TOF in positive electrospray ionization mode and spectra were recorded using sodium formate solution as the calibrant. Elemental analyses were performed by Mr. Stephen Boyer, London Metropolitan University.

Synthesis of Ligands and Precursors

2,2'-(phenylmethylene)dipyridine (pmdp, L1)

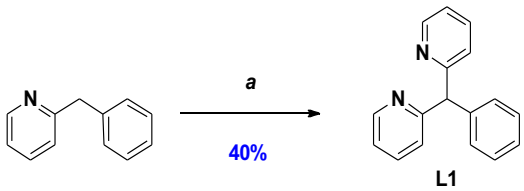

Chart **S1**. Synthesis route for 2,2'-(phenylmethylene)dipyridine, **L1**; (a) i) THF, *n*-BuLi, N_2, -78 °C, 1 h; ii) 2-fluoropyridine, THF, -78 °C to r.t., 18 h. (iii) reflux, 3 h.

2,2'-(phenylmethylene)dipyridine (pmdp, **L1**) was obtained following a modification of a reported procedure.[1] A solution of 2-benzylpyridine (1.763 g, 10.42 mmol, 1.0 equiv.) in dry THF (80 mL) was cooled down in an acetone/dry ice bath to -78 °C. n-BuLi (2.5 M in hexanes; 5 mL, 12.50 mmol, 1.2 equiv.) was added carefully resulting in the colour to change immediately to red. The solution was stirred at that temperature for 1 h. 2-fluoropyridine (1.517 g, 15.63 mmol, 1.5 equiv.) was then added carefully. After 1 h the cooling bath was removed and stirring was continued. After 18 h the reaction mixture was heated to 60 °C for 3 h and was then allowed to cool to room temperature and was quenched carefully with water (20 mL). 1 M HCl was added until pH neutral. The mixture was extracted with Et_2O and the organic layer was washed with brine and dried over $MgSO_4$. The solvent was evaporated leaving brown oil, which was purified over silica (10-100% EtOAc in hexanes). The desired fractions were combined, and the solvent evaporated leaving a beige solid (1.038 g, 4.21 mmol). **Yield:** 40%. **R_f:** 0.45 (100% EtOAc on silica). **Mp.:** 94–98 °C. **Lit**:[2] 95–97 °C. **^{1}H NMR (400 MHz, $CDCl_3$) δ (ppm):** 8.58 (ddd, J = 4.9, 2.0, 0.9 Hz, 2H), 7.62 (td, J = 7.7, 1.9 Hz, 2H), 7.34 – 7.26 (m, 4H), 7.24 (dq, J = 7.8, 1.2 Hz, 3H), 7.14 (ddd, J = 7.5, 4.9, 1.2 Hz, 2H), 5.82 (s, 1H).

^{13}C NMR (126 MHz, $CDCl_3$) δ (ppm): 162.20, 149.47, 141.73, 136.66, 129.41, 128.65, 126.89, 124.19, 121.68, 61.77. **HR-MS** ($FTMS^+$)**: $[M-H]^+$ Calculated:** ($C_{17}H_{14}N_2H$): 247.1230; **Found:** 247.1230. The characterization matches that previously reported.[2]

General procedure for the Synthesis of target Complexes

Iridium(III) chloride (2.0 equiv.) and the corresponding cyclometalating ligand (5.0 equiv.) were suspended in a mixture of 2-ethoxyethanol/water (75/25). The mixture was heated to and kept at 125 °C with stirring. After 24 h the mixture was allowed to cool to r.t. and distilled water (5 mL) was added giving a precipitate. This was washed with H_2O, Et_2O, and dried under vacuum to give the intermediate bis(μ-Cl)dimer complex. A suspension of this dimer (1.0 equiv.), the ancillary ligand 2,2'-(phenylmethylene)dipyridine (2.2 equiv.) in a 1:2 mixture of CH_2Cl_2/MeOH was refluxed with stirring for 18 h. The solvent was then evaporated leaving a yellow residue, which was purified over silica with dichloromethane and increasing percentage of methanol (0% - 8%). The desired fractions were collected and reduced to dryness giving a yellow solid which was dissolved in methanol. An aqueous solution of NH_4PF_6 (1.00 g in 10 mL of H_2O) was slowly added. A yellow precipitate was observed. The suspension was stirred vigorously for 2 h. The precipitate was filtered off, washed with water and Et_2O and recrystallized in a CH_2Cl_2/hexane mixture at -20 °C. After filtration, the desired compound was obtained as a yellow solid. Complex **1**

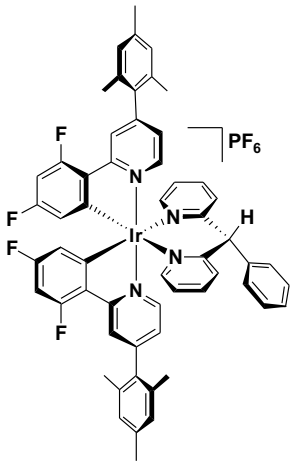

Yellow solid. **Yield:** 81%. **Mp.:** 282 °C (decomp.). **^{1}H NMR (400 MHz, $CDCl_3$) δ (ppm):** 8.40 (d, J = 5.8 Hz, 1H), 8.16 (d, J = 8.7 Hz, 2H), 8.07 – 7.95 (m, 5H), 7.35 (dt, J = 18.3, 5.5 Hz, 3H), 7.19 – 7.13 (m, 4H), 7.02 – 6.95 (m, 5H), 6.68 (d, J = 7.1 Hz, 2H), 6.51 (dd, J = 16.8, 9.2 Hz, 2H), 6.36 – 6.30 (m, 2H), 5.64 (dd, J = 8.6, 2.3 Hz, 1H), 5.23 (dd, J = 8.8, 2.3 Hz, 1H), 2.35 (s, 6H), 2.13 (d, J = 3.2 Hz, 6H), 2.01 (s, 3H), 1.96 (s, 3H). **^{13}C NMR (126 MHz, $CDCl_3$) δ (ppm):** 164.05, 164.00, 163.79, 163.74, 162.27, 158.23, 157.97, 153.50, 152.77, 152.58, 152.44, 152.32, 151.71, 151.66, 151.44, 151.39, 150.46, 149.19, 140.33, 139.91, 139.66, 138.57, 138.48, 134.98, 134.93, 134.71, 134.54, 130.48, 130.35, 129.33, 128.71, 128.17, 125.85, 125.36, 125.24, 125.16, 124.54, 124.39, 123.93, 114.08, 113.10, 99.53, 59.86, 21.09, 20.72, 20.57, 20.49, 20.38. **^{19}F NMR (376 MHz, $CDCl_3$) δ (ppm):** -72.20, -73.71, -105.23 (dd, *J* = 33.5, 28.6 Hz), -107.28 (d, *J* = 23.3 Hz), -107.98 (d, *J* = 23.3 Hz). **^{31}P NMR (162 MHz, $CDCl_3$) δ (ppm):** -144.72. **HR-MS** ($FTMS^{+}$)**: $[M]^{+}$ Calculated:** ($C_{57}H_{46}F_6IrN_4$): 1055.3287; **Found:** 1055.3272. **CHN**: **Calcd.** for $C_{57}H_{46}F_{10}IrN_4P$: C, 57.04; H, 3.86; N, 4.67. **Found:** C, 57.12; H, 4.04; N, 4.58.

Complex **2**

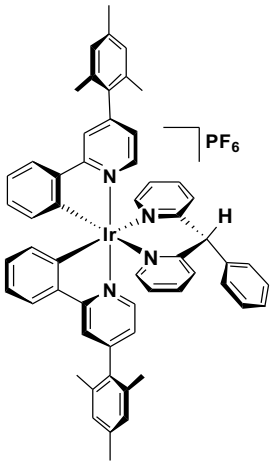

Yellow solid. **Yield:** 89%. **Mp.:** 260 °C (decomp.). **^{1}H NMR (400 MHz, $CDCl_3$) δ (ppm):** 8.50 (d, J = 6.2 Hz, 1H), 8.16 – 8.10 (m, 2H), 8.08 – 7.96 (m, 3H), 7.74 (d, J = 1.8 Hz, 1H), 7.62 (d, J = 1.9 Hz, 1H), 7.58 (td, J = 8.0, 1.3 Hz, 2H), 7.38 (t, J = 6.2 Hz, 2H), 7.28 – 7.24 (m, 1H), 7.19 (q, J = 7.2, 6.2 Hz, 3H), 7.10 (ddd, J = 7.3, 5.9, 1.3 Hz, 1H), 7.05 – 6.99 (m, 5H), 6.99 – 6.94 (m, 2H), 6.94 – 6.90 (m, 1H), 6.84 (td, J = 7.7, 1.1 Hz, 1H), 6.73 (d, J = 7.1 Hz, 2H), 6.35 – 6.29 (m, 2H), 6.29 – 6.25 (m, 1H), 5.91 (d, J = 7.6 Hz, 1H), 2.38 (s, 6H), 2.16 (d, J = 11.3 Hz, 6H), 2.06 (s, 3H), 1.98 (s, 3H). **^{13}C NMR (126 MHz, $CDCl_3$) δ (ppm):** 167.81, 167.37, 158.56, 158.26, 153.34, 152.84, 152.47, 151.29, 150.48, 149.09, 148.22, 147.78, 144.29, 144.08, 139.93, 139.54, 138.60, 138.49, 135.14, 135.08, 134.97, 134.89, 131.96, 130.90, 130.84, 130.75, 129.94, 129.80, 129.37, 128.85, 128.74, 128.45, 128.19, 125.63, 125.14, 124.97, 124.85, 124.52, 123.73, 122.99, 122.91, 121.18, 120.71, 60.18, 21.22, 20.84, 20.71, 20.59, 20.49. **^{31}P NMR (162 MHz, $CDCl_3$) δ (ppm):** 144.46. **HR-MS** ($FTMS^{+}$)**: $[M]^{+}$ Calculated:** ($C_{57}H_{50}IrN_4$): 983.3664; **Found:** 983.3656. **CHN**: **Calcd.** for $C_{57}H_{50}F_6IrN_4P$ x 5/2 CH_2Cl_2: C, 53.31; H, 4.14; N, 4.18. **Found:** C, 53.08; H, 4.27; N, 4.45.

Characterization of 2,2'-(phenylmethylene)dipyridine (pmdp) and complexes 1-2

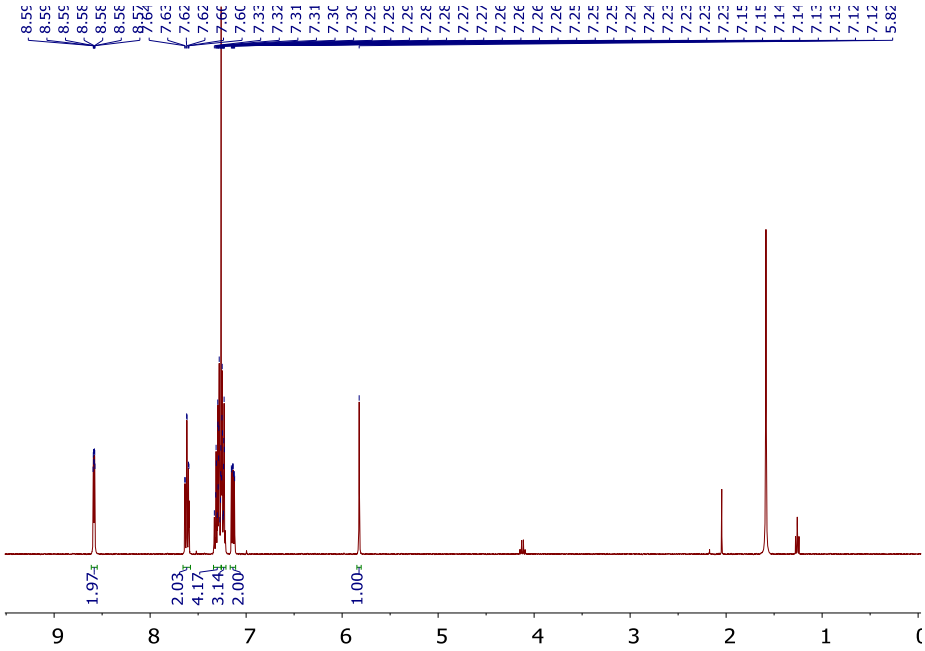

Figure **S1.** ^{1}H NMR spectrum of 2,2'-(phenylmethylene)dipyridine (pmdp) in $CDCl_3$

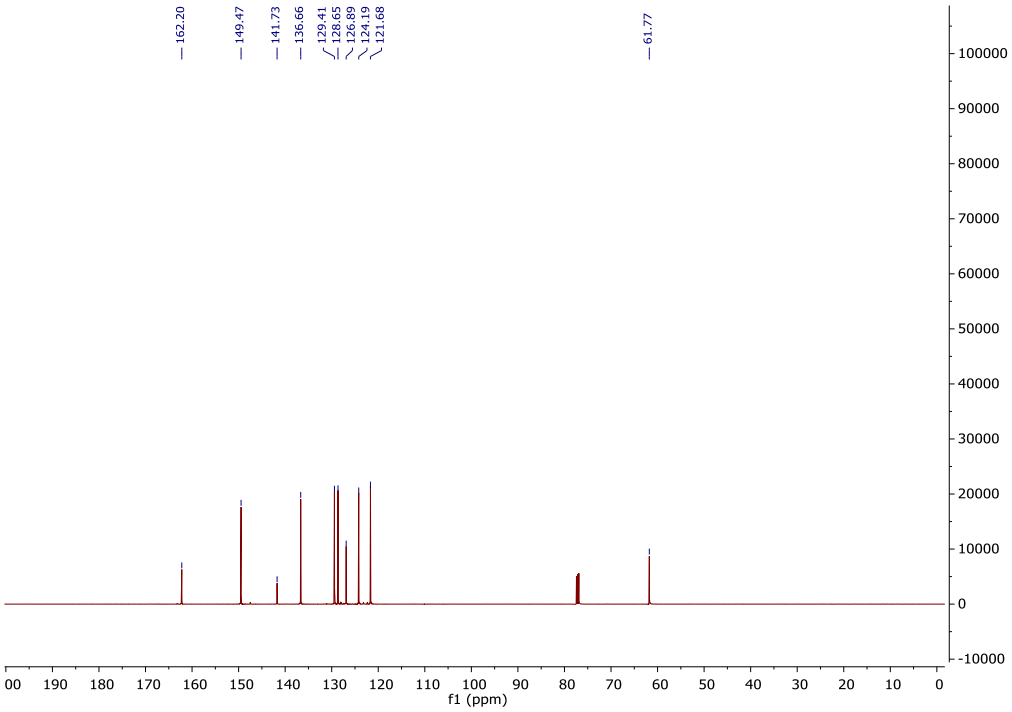

Figure **S2.** ^{13}C NMR spectrum of 2,2'-(phenylmethylene)dipyridine (pmdp) in $CDCl_3$

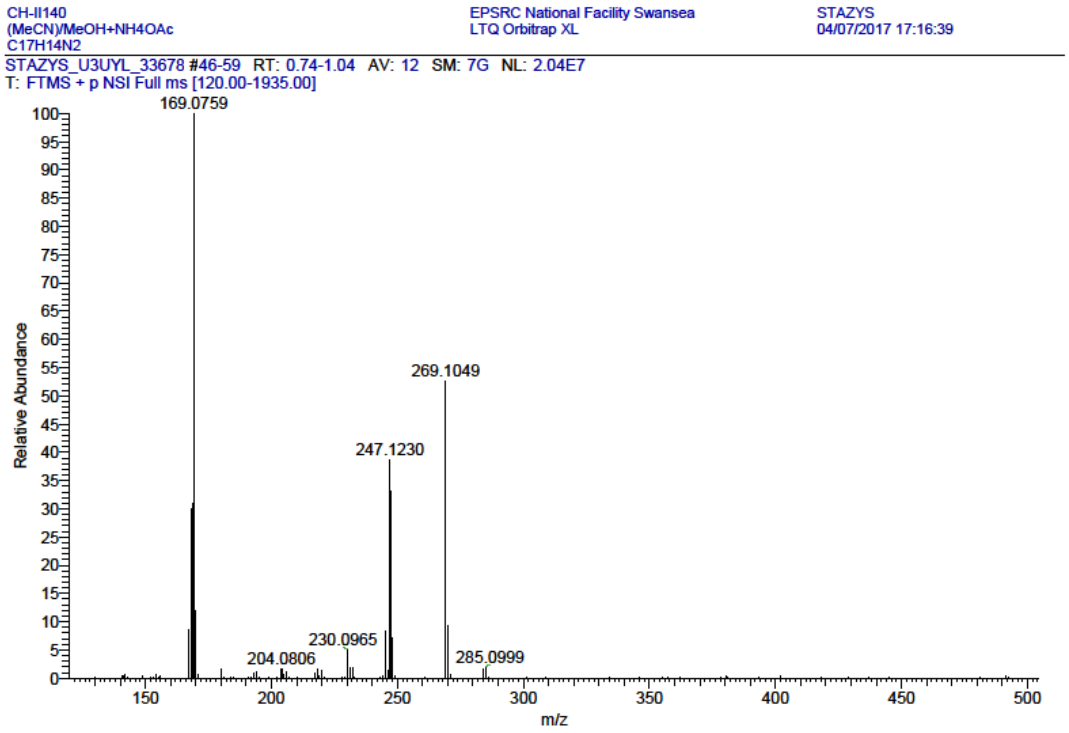

Figure **S3**. FT mass spectrum of 2,2'-(phenylmethylene)dipyridine (pmdp)

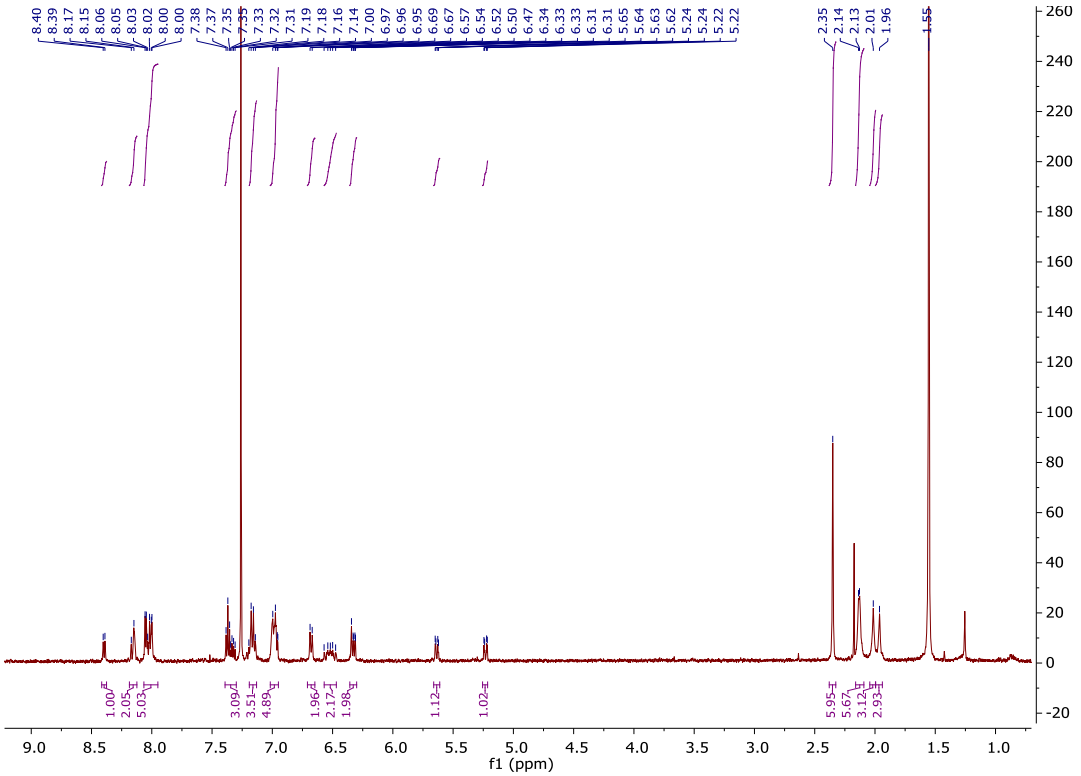

Figure **S4.** ^{1}H NMR spectrum of [Ir(dFMesppy)$_2$(pmdp)](PF$_6$) (**1**) in CDCl$_3$

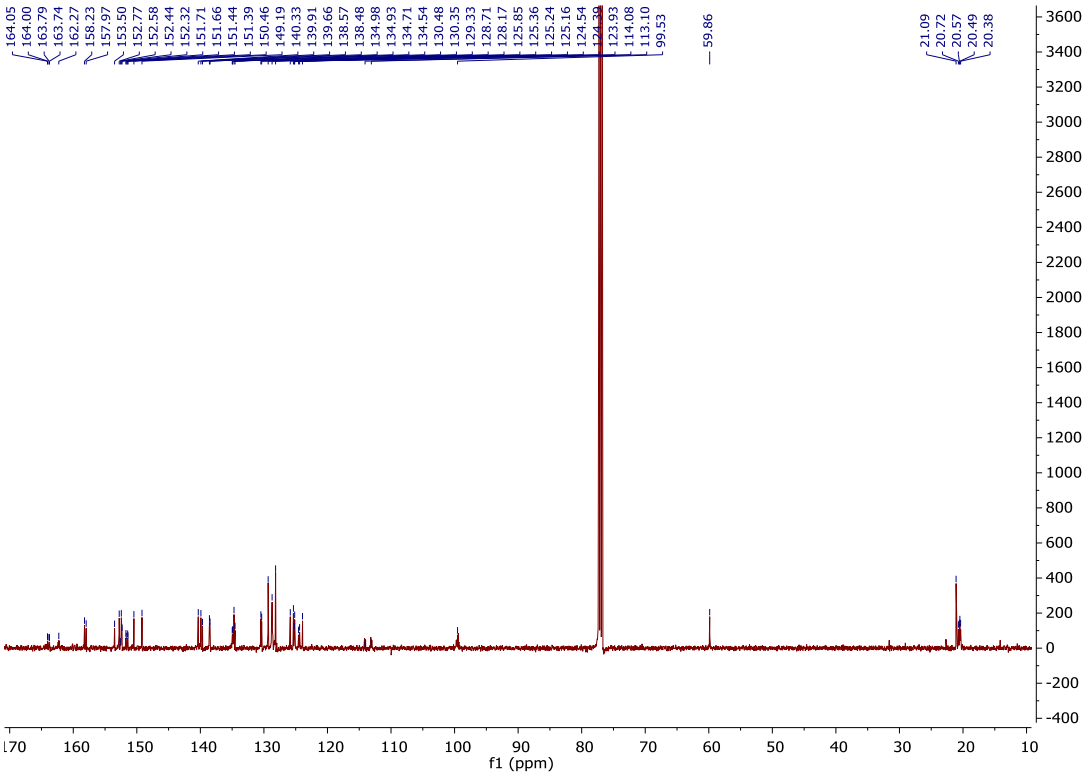

Figure **S5.** ^{13}C NMR spectrum of $[Ir(dFMesppy)_2(pmdp)](PF_6)$ (**1**) in $CDCl_3$

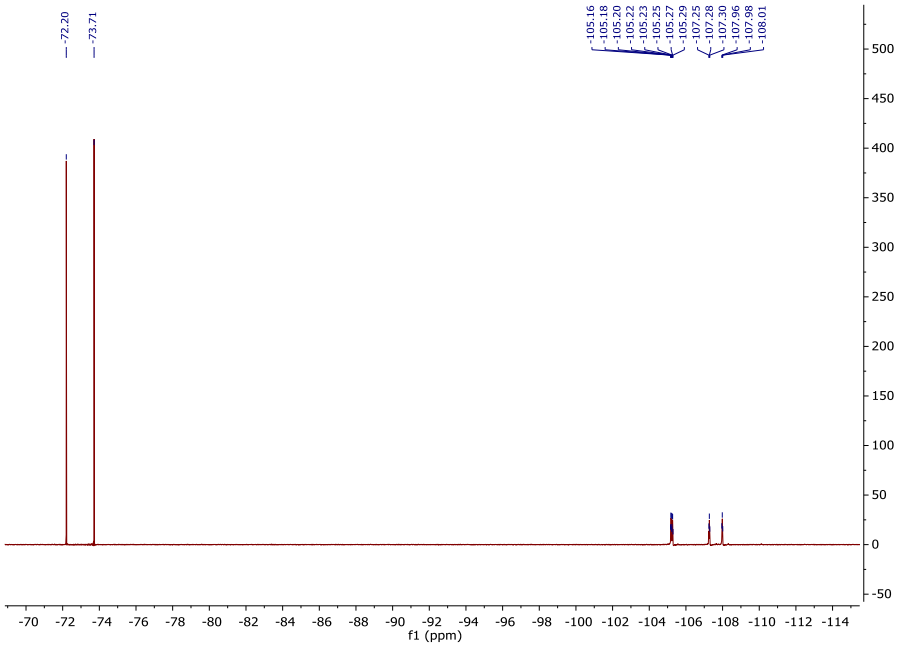

Figure **S6.** ^{19}F NMR spectrum of $[Ir(dFMesppy)_2(pmdp)](PF_6)$ (**1**) in $CDCl_3$

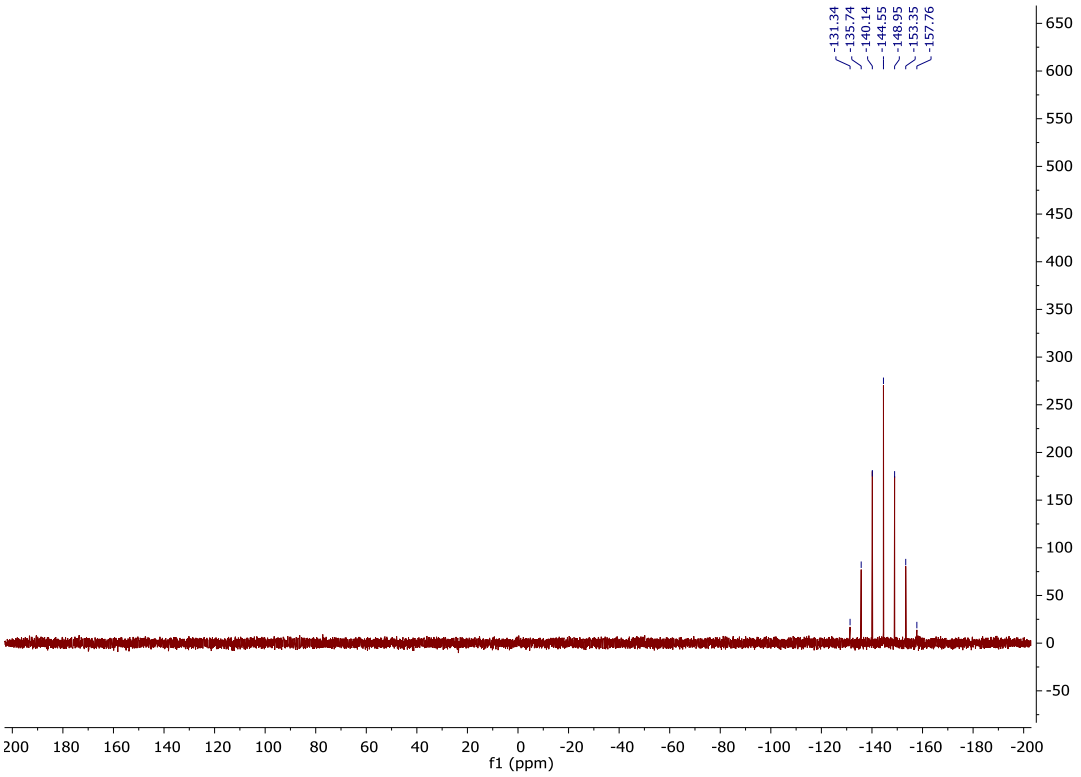

Figure **S7.** ^{31}P NMR spectrum of [Ir(dFMesppy)$_2$(pmdp)](PF$_6$) (**1**) in CDCl$_3$

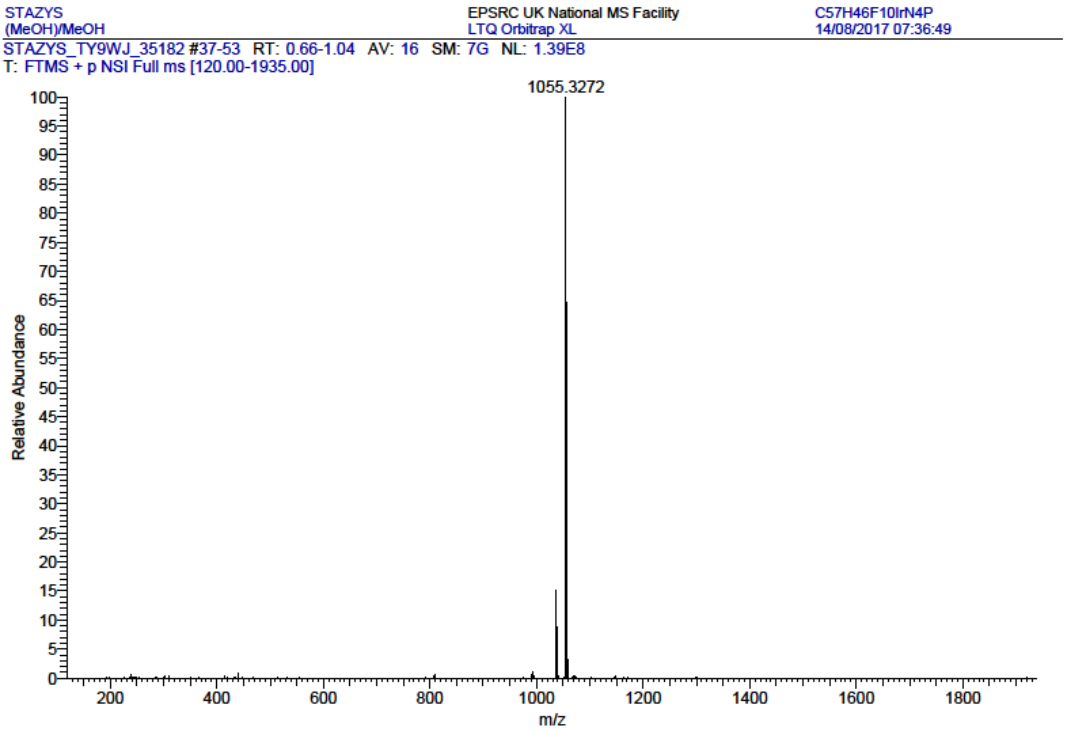

Figure **S8**. FT mass spectrum of [Ir(dFMesppy)$_2$(pmdp)](PF$_6$) (**1**)

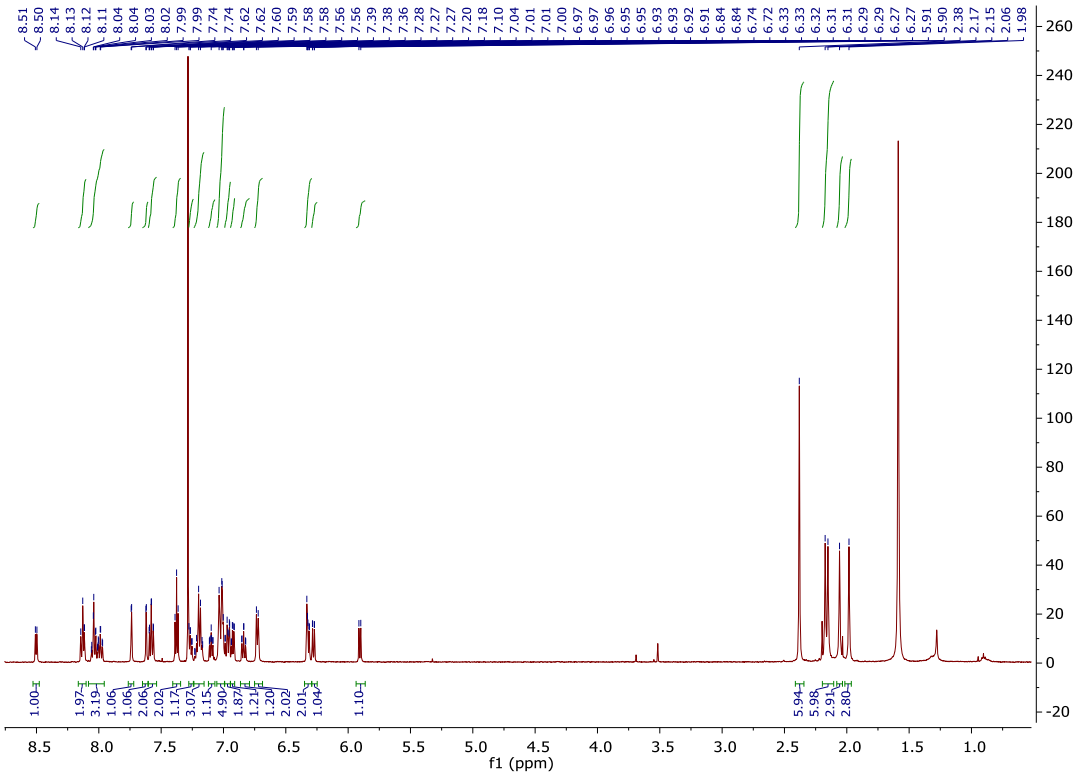

Figure **S9.** ^{1}H NMR spectrum of [Ir(Mesppy)$_2$(pmdp)](PF$_6$) (**2**) in CDCl$_3$

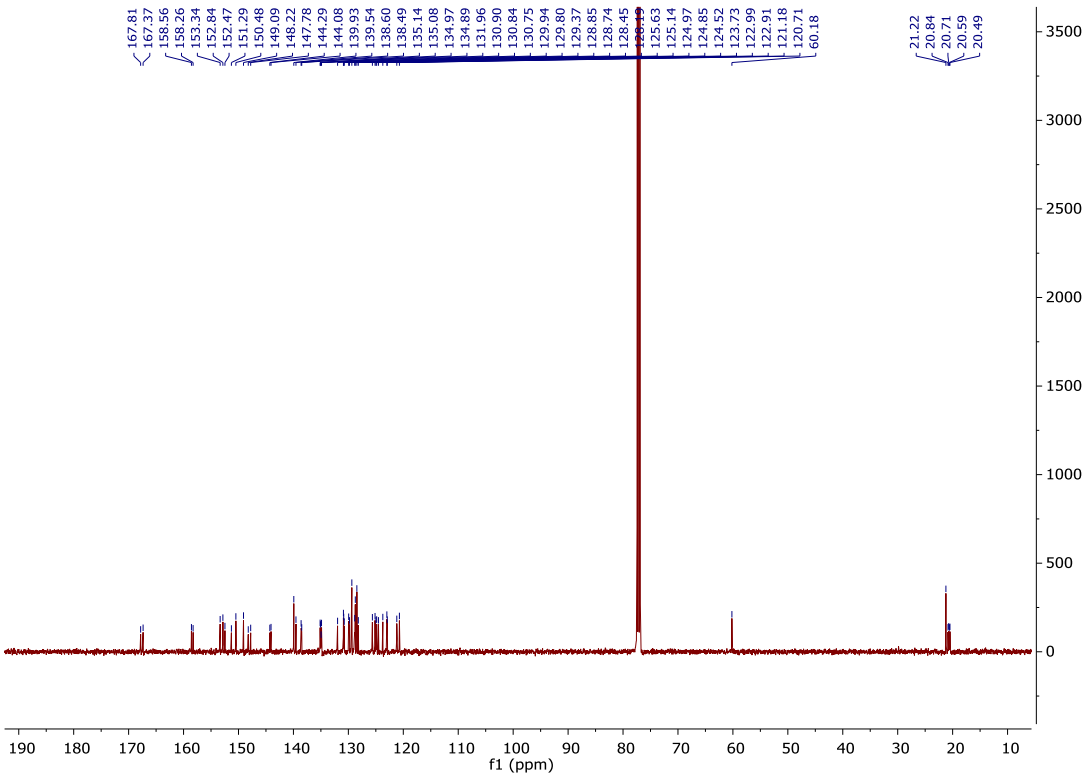

Figure **S10.** ^{13}C NMR spectrum of [Ir(Mesppy)$_2$(pmdp)](PF$_6$) (**2**) in CDCl$_3$

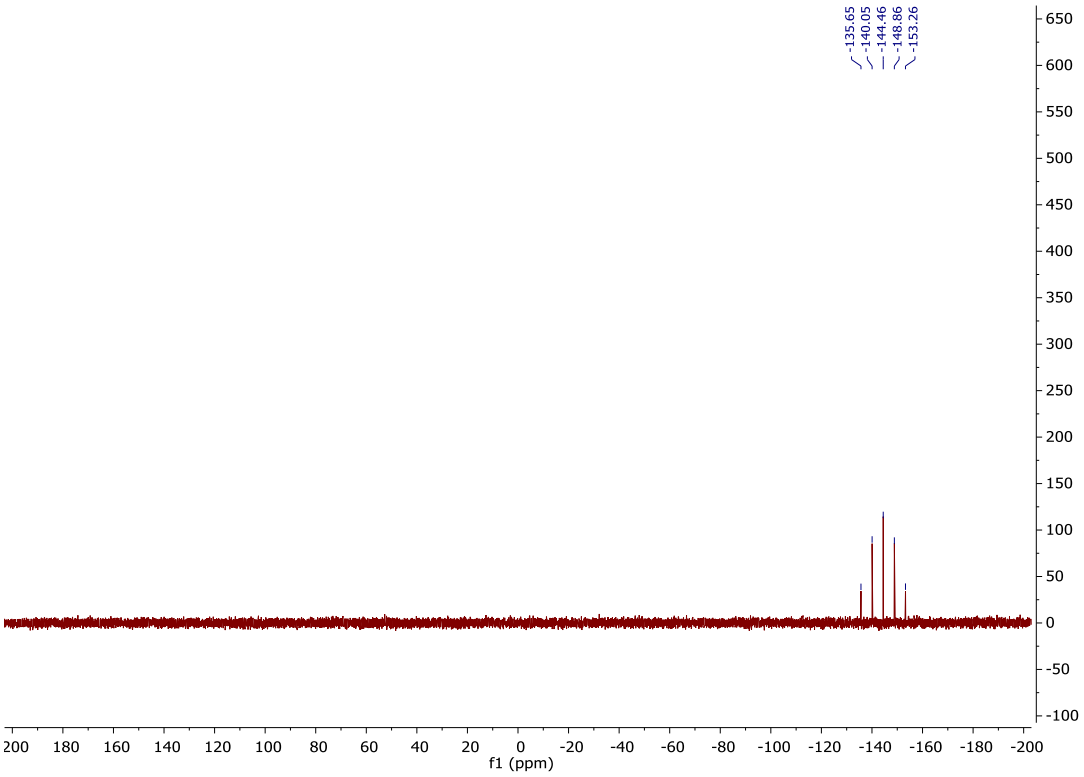

Figure **S11.** ^{31}P NMR spectrum of [Ir(Mesppy)$_2$(pmdp)](PF$_6$) (**2**) in CDCl$_3$

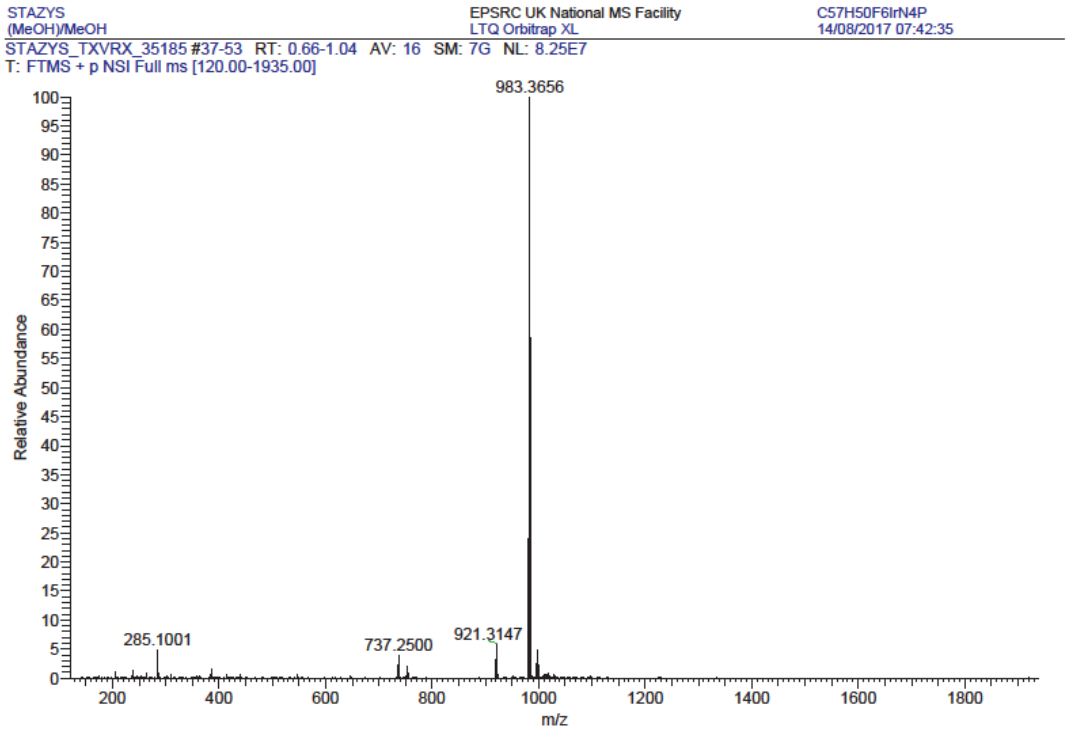

Figure **S12**. FT mass spectrum of [Ir(Mesppy)$_2$(pmdp)](PF$_6$) (**2**)

X-ray crystal structures

Single crystals of sufficient quality of **1** were grown from CH_2Cl_2/hexane via vapor diffusion. X-ray diffraction data for were collected at 173 K by using a Rigaku FR-X Ultrahigh Brilliance Microfocus RA generator/confocal optics with XtaLAB P200 diffractometer [Mo Kα radiation (λ = 0.71075 Å)]. Intensity data were collected using ω steps accumulating area detector images spanning at least a hemisphere of reciprocal space. All data were corrected for Lorentz polarization effects. A multiscan absorption correction was applied by using CrystalClear.[3] The structure was solved by Patterson methods (PATTY[4]) and refined by full-matrix least-squares against F^2 (SHELXL-2016[5]). Non-hydrogen atoms were refined anisotropically, and hydrogen atoms were refined using a riding model. All calculations were performed using the CrystalStructure[6] interface. Selected crystallographic data are presented in Table S1. CCDC 1821381 contains the supplementary crystallographic data for this paper. The data can be obtained free of charge from The Cambridge Crystallographic Data Centre via www.ccdc.cam.ac.uk/structures.

Table S1. Selected crystallographic parameters for complex **1**

	1
empirical formula	C58 H48 Cl2 F10 Ir N4 P
fw	1285.13
crystal description	yellow needle
crystal dimensions [mm^3]	0.45×0.03×0.03
space group	$P2_1/n$ (No. 14)
a [Å]	10.9755(10)
b [Å]	19.9924(18)
c [Å]	24.106(2)
β [°]	99.867(3)
vol $[Å]^3$	5211.3(8)
Z	4
ρ (calc) [g/cm^3]	1.683
μ [mm^{-1}]	2.782
F(000)	2560
reflns collected	62738

independent reflns (R_{int})	9498 (0.0604)
data/restraints/params	9498/9/691
GOF on F^2	1.041
R_1 [$I > 2\sigma(I)$]	0.0360
wR_2 (all data)	0.0793
largest diff. peak/hole [e/Å^3]	1.35, -1.22

Electrochemistry

Cyclic and differential pulse voltammetry measurements were performed on an Electrochemical Analyzer potentiostat model 600D from CH Instruments. Solutions for cyclic voltammetry were prepared in MeCN and degassed with MeCN-saturated nitrogen by bubbling for about 10 min prior to scanning. Tetra(*n*-butyl)ammoniumhexafluorophosphate ([TBA](PF$_6$); ca. 0.1 M in MeCN) was used as the supporting electrolyte. Two Ag/Ag$^+$ electrode (silver wire in a solution of 0.1 M KCl in H_2O) were used as the pseudoreference electrode and counter electrode, respectively; a platinum electrode was used for the working electrode. The redox potentials are reported relative to a saturated calomel electrode (SCE) electrode with a ferrocene/ferrocenium (Fc/Fc$^+$) redox couple as an internal reference (0.38 V vs. SCE).[7]

Photophysical data

All samples were prepared in HPLC grade MeCN with varying concentrations in the order of micromolar. Absorption spectra were recorded at room temperature using a Shimadzu UV-1800 double beam spectrophotometer. Molar absorptivity determination was verified by linear least-squares fit of values obtained from at least four independent solutions at varying concentrations ranging from 3.10×10^{-5} to 4.87×10^{-6} M. The sample solutions for the emission spectra were prepared in HPLC grade MeCN and degassed via three freeze−pump−thaw cycles using an in-house designed quartz cuvette. Steady-state and time-resolved emission spectra were recorded

at room temperature using Gilden photonics Fluorimeter. For steady-state measurements at room temperature complexes **1** and **2** were excited at 360 nm. The excited-state lifetimes of the complexes were obtained by time correlated single photon counting (TCSPC) at an excitation wavelength of 378 nm using an Edinburgh Instruments FLS980 fluorimeter using a pulsed diode laser, and PL emission was detected at the corresponding steady-state emission maximum for each complex. The PL decays were fitted with a multi exponential decay function. Emission quantum yields were determined using the optically dilute method.[8] A stock solution with absorbance of ca. 0.2 was prepared, and then four dilutions were prepared with dilution factors ranging from 2 to 20 to obtain solutions with absorbances of ca. 0.106, 0.075, 0.050, and 0.025, respectively. The Beer−Lambert law was found to be respected (linear dependency) at the concentrations of the solutions. The emission spectra were then measured after the solutions were degassed by three freeze−pump−thaw cycles using an in-house designed quartz cuvette prior to spectrum acquisition. For each sample, linearity between absorption and emission intensity was verified through linear regression analysis, and additional measurements were acquired until the Pearson regression factor (R^2) for the linear fit of the data set surpassed 0.9. Individual relative quantum yield values were calculated for each solution, and the values reported represent the slope value. The $\Phi_s = \Phi_r(A_r/A_s)(I_s/I_r)(n_s/n_r)^2$ equation was used to calculate the relative quantum yield of each of the sample, where Φ_r is the absolute quantum yield of the reference, n is the refractive index of the solvent, A is the absorbance at the excitation wavelength, and I is the integrated area under the corrected emission curve. The subscripts s and r refer to the sample and reference, respectively. A solution of Quinine sulfate in 0.5 M H_2SO_4 was used as the reference (Φ_{PL} = 54.6% at 298 K).[9]

Table **S2**. Selected photophysical data for complexes **1-2**.

[a] recorded in aerated MeCN at 298 K

	λ_{abs} / nm (ε / $M^{-1}cm^{-1}$)[a]
1	264 (44 534), 313 (20 451), 368 (6 475), 431 (1 044)
2	269 (39 166), 344 (9 168), 384 (4 932), 443 (638)

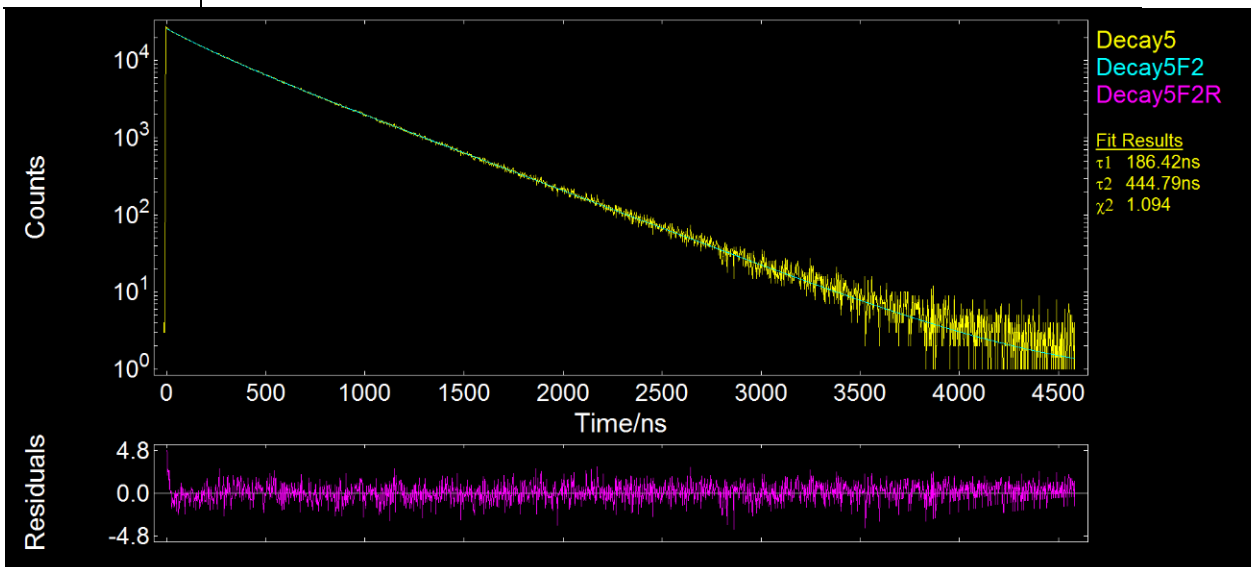

Figure **S13**. Excited-state lifetime (λ_{exc} = 378 nm) decay profile of **1** in deaerated MeCN at room temperature

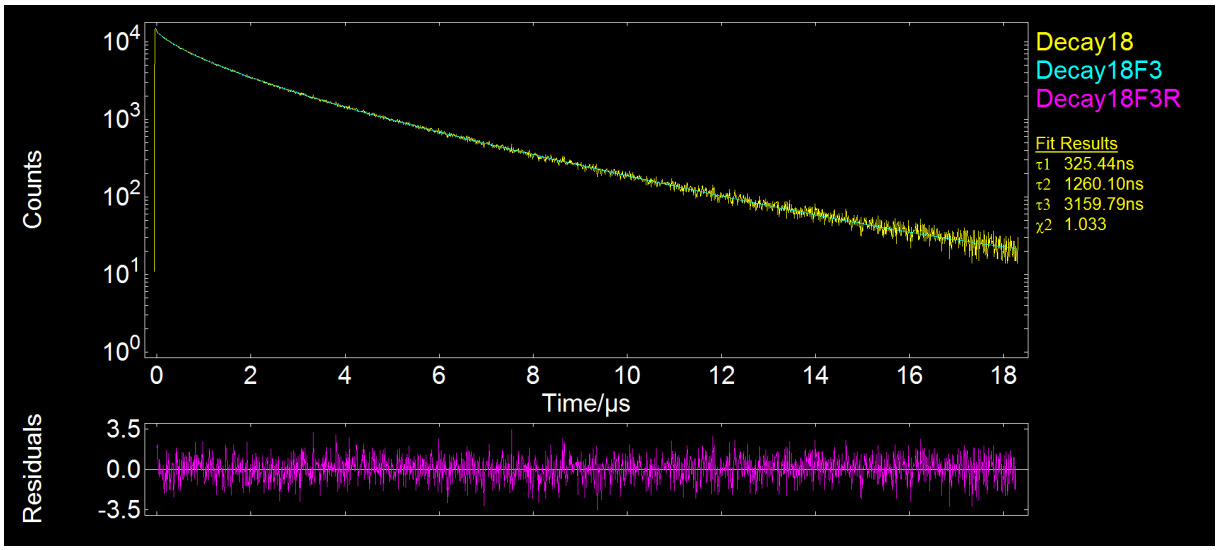

Figure **S14**. Excited-state lifetime (λ_{exc} = 378 nm) decay profile of **1** in PMMA film (5 wt% of the complex in PMMA) at room temperature

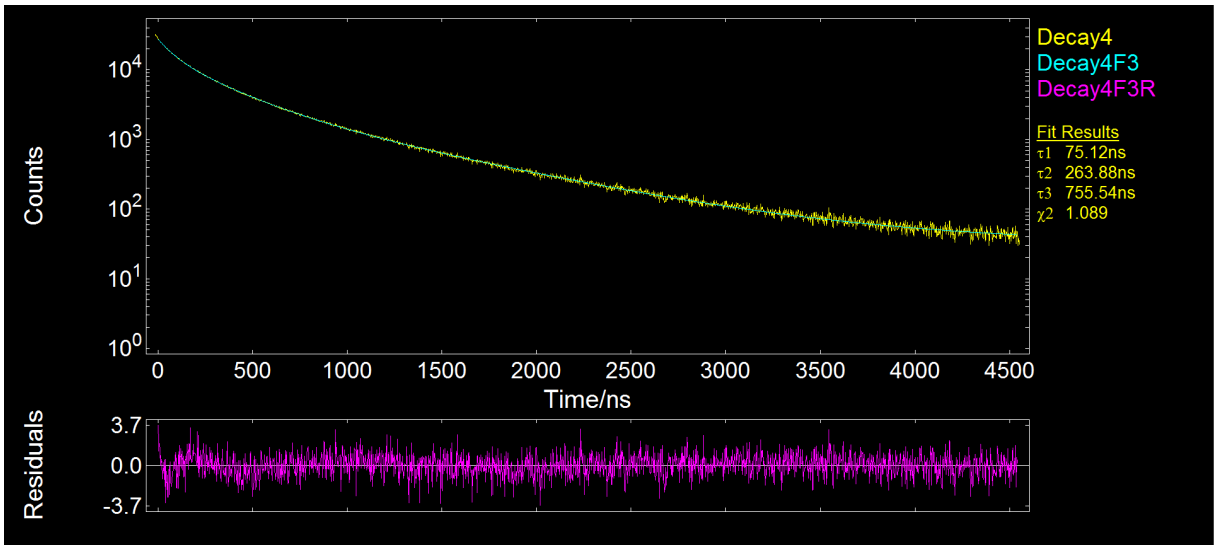

Figure **S15**. Excited-state lifetime (λ_{exc} = 378 nm) decay profile of **1** in neat film (spin-coated) at room temperature

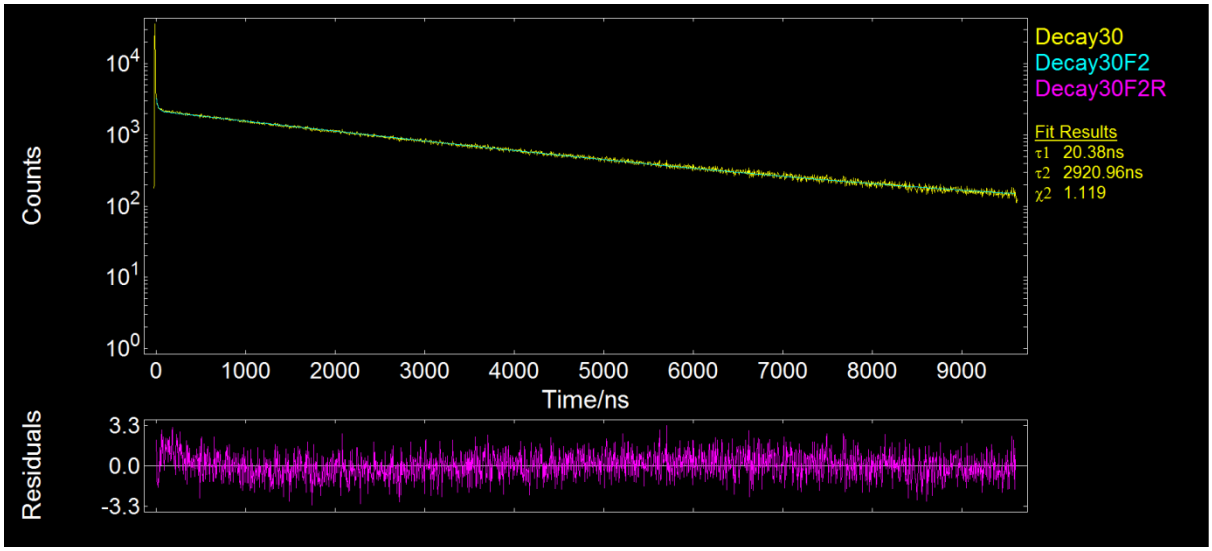

Figure **S16**. Excited-state lifetime (λ_{exc} = 378 nm) decay profile of **1** in 2-MeTHF Glass at 77 K

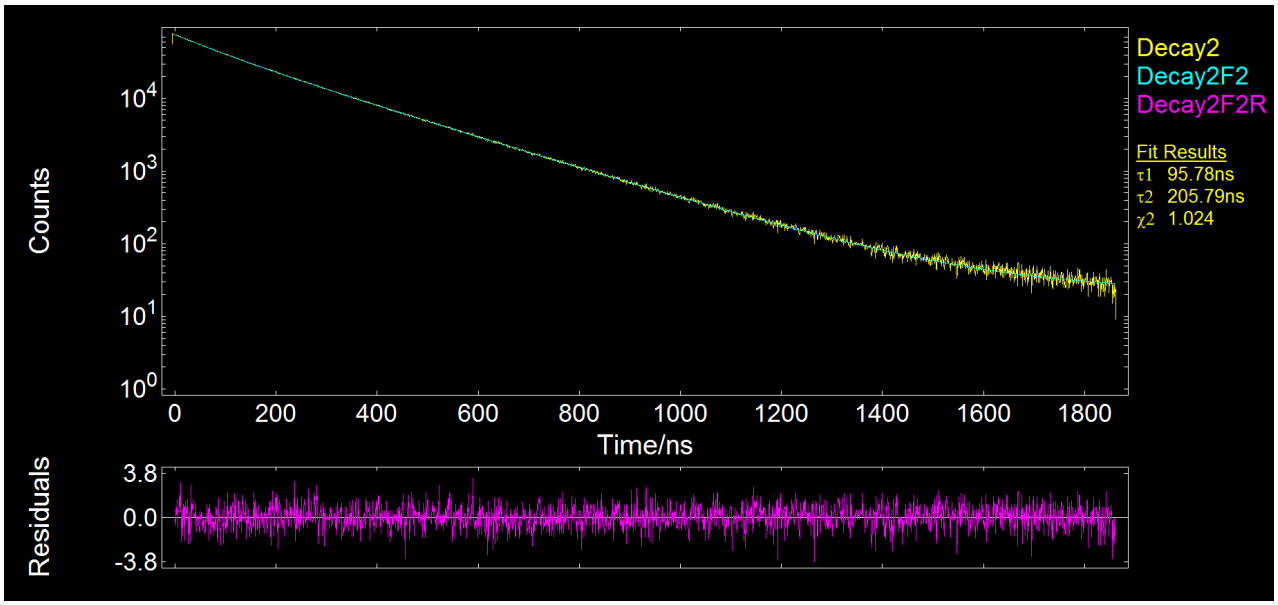

Figure **S17**. Excited-state lifetime (λ_{exc} = 378 nm) decay profile of **2** in deaerated MeCN at room temperature

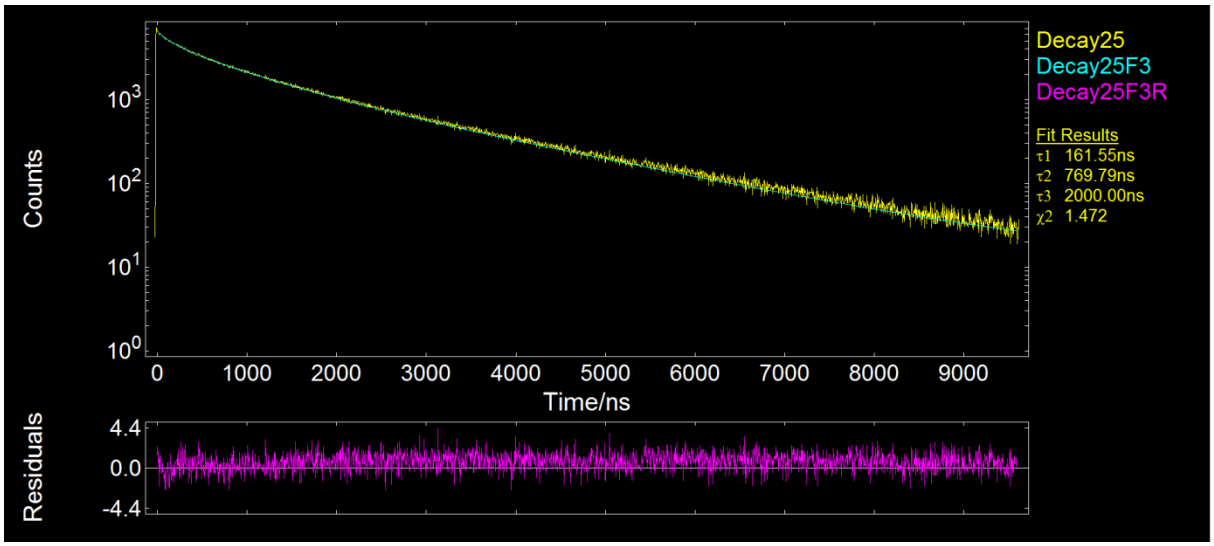

Figure **S18**. Excited-state lifetime (λ_{exc} = 378 nm) decay profile of **2** in PMMA film (5 wt% of the complex in PMMA) at room temperature

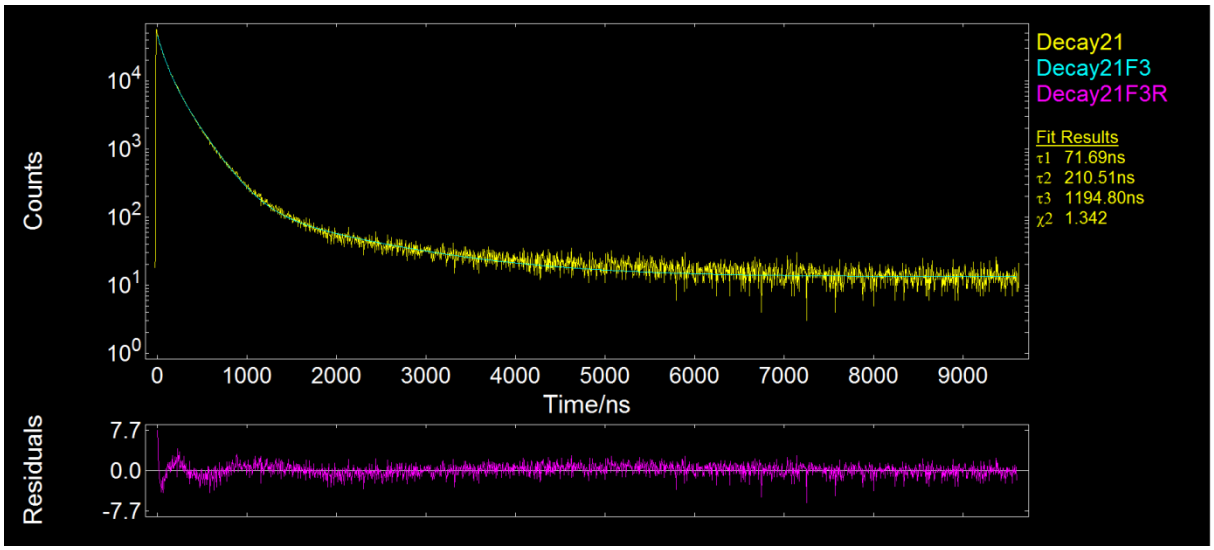

Figure **S19.** Excited-state lifetime (λ_{exc} = 378 nm) decay profile of **2** in neat film (spin-coated) at room temperature

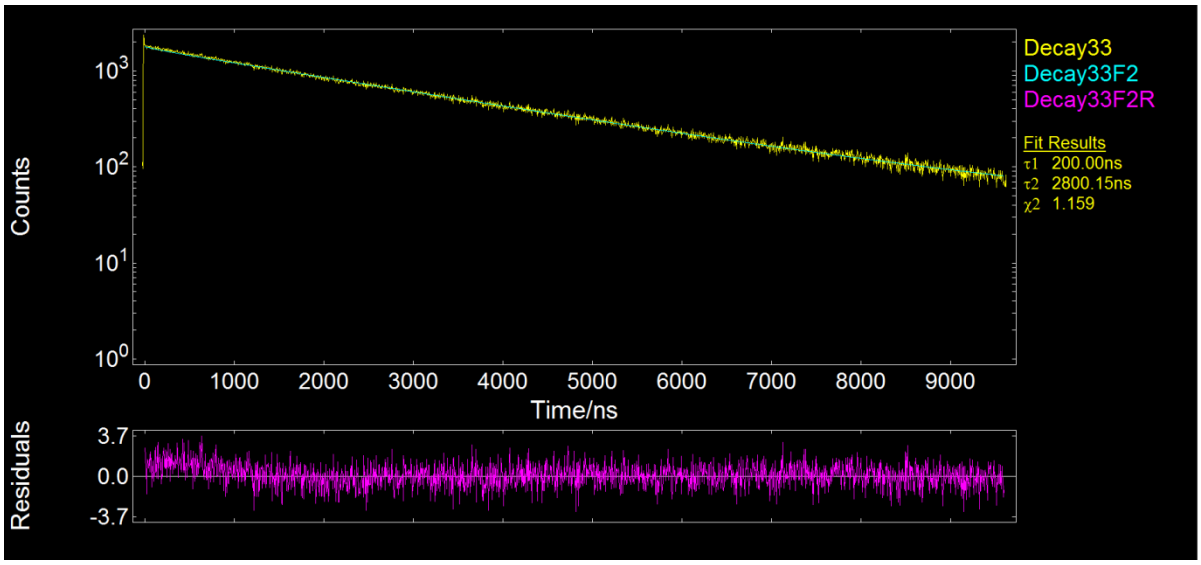

Figure **S20**. Excited-state lifetime (λ_{exc} = 378 nm) decay profile of **2** in 2-MeTHF Glass at 77 K

Theoretical calculations

To perform our simulations, we have selected the latest version of the Gaussian program.[10] The *ab initio* simulations consisted in geometry optimization of both the lowest singlet and triplet states, and subsequent TD-DFT calculations performed on the ground-state structures. We have applied default procedures, integration grids, algorithms and parameters, except for tighten energy (typically 10^{-10} *a.u.*) and internal forces (10^{-5} *a.u.*) convergence thresholds and the use of the *ultrafine* integration DFT grid. The ground-state geometrical parameters have been determined with the M06 functional.[11] The vibrational spectrum has been subsequently determined analytically at the same level of theory and it has been checked that all structures correspond to true minima of the potential energy surface. At least, the first forty low-lying excited-states have been determined within the vertical TD-DFT approximation using the same functional that again is pertinent for absorption spectra.[12] For all nuclei, we have used the LanL2DZ(5*d*,7*f*) basis set and pseudopotential augmented by additional *d* (C, N, F) and *f* (Ir) functions of contraction length one (α=0.938, 0.587, 0.736, and 1.577 for Ir, C, N and F, respectively). During all steps, a modelling of bulk solvent effects (here acetonitrile) through the Polarizable Continuum Model (PCM),[13] using the liner-response approach for the TD-DFT part of the calculation. The isovalue for representation was set to 0.03 au. for the MOs.

References

(1). A. Santoro, C. Sambiagio, P. C. McGowan and M. A. Halcrow, *Dalton Trans*, 2015, **44**, 1060-1069.

(2). T. Niwa, H. Yorimitsu and K. Oshima, *Org. Lett.*, 2007, **9**, 2373-2375.

(3). *CrystalClear-SM Expert v. 2.1;* , Rigaku Americas, Rigaku Americas, The Woodlands, Texas, USA and Rigaku Corporation, Tokyo, Japan, 2015.

(4). P. T. Beurskens, G. Beurskens, R. de Gelder, S. Garcia-Granda, R. O. Gould, R. Israel and J. M. M. Smits, Crystallography Laboratory, University of Nijmegen, The Netherlands, 1999.

(5). G. Sheldrick, *Acta Crystallogr., Sect. C: Cryst. Struct. Commun.*, 2015, **71**, 3-8.

(6). *CrystalStructure v4.2.*, The Woodlands, Texas, USA and Rigaku Corporation, Tokyo, Japan, 2015.

(7). V. V. Pavlishchuk and A. W. Addison, *Inorg. Chim. Acta*, 2000, **298**, 97-102.

(8). G. A. Crosby and J. N. Demas, *J. Phys. Chem.*, 1971, **75**, 991-1024.

(9). W. H. Melhuish, *J. Phys. Chem.*, 1961, **65**, 229-235.

(10). M. J. Frisch, G. W. Trucks, H. B. Schlegel, G. E. Scuseria, M. A. Robb, J. R. Cheeseman, G. Scalmani, V. Barone, G. A. Petersson, H. Nakatsuji, X. Li, M. Caricato, A. V. Marenich, J. Bloino, B. G. Janesko, R. Gomperts, B. Mennucci, H. P. Hratchian, J. V. Ortiz, A. F. Izmaylov, J. L. Sonnenberg, Williams, F. Ding, F. Lipparini, F. Egidi, J. Goings, B. Peng, A. Petrone, T. Henderson, D. Ranasinghe, V. G. Zakrzewski, J. Gao, N. Rega, G. Zheng, W. Liang, M. Hada, M. Ehara, K. Toyota, R. Fukuda, J. Hasegawa, M. Ishida, T. Nakajima, Y. Honda, O. Kitao, H. Nakai, T. Vreven, K. Throssell, J. A. Montgomery Jr., J. E. Peralta, F. Ogliaro, M. J. Bearpark, J. J. Heyd, E. N. Brothers, K. N. Kudin, V. N. Staroverov, T. A. Keith, R. Kobayashi, J. Normand, K. Raghavachari, A. P. Rendell, J. C. Burant, S. S. Iyengar, J. Tomasi, M. Cossi, J. M. Millam, M. Klene, C. Adamo, R. Cammi, J. W. Ochterski, R. L. Martin, K. Morokuma, O. Farkas, J. B. Foresman and D. J. Fox, Wallingford, CT, 2016.

(11). Y. Zhao and D. G. Truhlar, *Theor. Chem. Acc.*, 2008, **120**, 215-241.

(12). (a) D. Jacquemin, E. A. Perpète, I. Ciofini, C. Adamo, R. Valero, Y. Zhao and D. G. Truhlar, *J. Chem. Theory Comput.*, 2010, **6**, 2071-2085; (b) D. Jacquemin, A. Planchat, C. Adamo and B. Mennucci, *J Chem Theory Comput*, 2012, **8**, 2359-2372.

(13). J. Tomasi, B. Mennucci and R. Cammi, *Chem. Rev.*, 2005, **105**, 2999-3094.